RESEARCH ARTICLE
eISSN 2234-1757
Fish Aquat Sci. 2026;29(8):532-538
https://doi.org/10.47853/FAS.2026.e45
FAS Fisheries and Aquatic Sciences

Four oxylipins from the brown alga *Eisenia bicyclis*

Gun-Woo Oh[1,#], Soo Jeong Lee[2,#], Dae-Cheol Choi[2], Seok-Chun Ko[1], Dongwoo Yang[1], Mi-Jin Yim[1], Dae-Sung Lee[1], Jeong Min Lee[1,*], Ji-Yul Kim[1,*]

[1] *National Marine Biodiversity Institute of Korea, Seocheon 33662, Korea*
[2] *Division of Biotechnology and Advanced Institute of Environmental and Bioscience, College of Environmental and Bioresource Sciences, Jeonbuk National University, Iksan 54596, Korea*

Abstract

Four oxylipin derivatives (1–4) were isolated from a 70% ethanol extract of *Eisenia bicyclis*, a brown alga. The structures of 1–4 were elucidated by the interpretation with nuclear magnetic resonance (NMR) and mass spectroscopic analysis. Compounds 1–4 were identified as (5*Z*,8*Z*,11*Z*,13*E*)-15-hydroxyicosa-5,8,11,13-tetraenoic acid, (5*Z*,8*Z*,11*Z*,13*E*,17*Z*)-15-hydroxyicosa-5,8,11,13,17-pentaenoic acid, (9*Z*,11*E*,15*Z*)-13-hydroxyoctadeca-6,9,11,15-trienoic acid, and (6*Z*,9*Z*,11*E*,15*Z*)-13-hydroxyoctadeca-6,9,11,15-tetraenoic acid, respectively. The compounds 1–4 were evaluated for their anti-inflammatory activity on the production of nitric oxide (NO) and cell viability at the concentrate of 100 μg/mL. These results showed that compound 4 exerted moderate inhibitory activity on NO production. Among compounds 1–4, compound 4 was found to be the most abundant, with a concentration of 0.161 ± 0.003 mg/g in the 70% ethanol extract of *E. bicyclis*.

Keywords: Anti-inflammatory activity, *Eisenia bicyclis*, Nuclear magnetic resonance (NMR), Multiple reaction monitoring (MRM)

Introduction

Eisenia bicyclis is an edible alga commonly used in South Korea and is distributed throughout the temperate regions of South Korea and Japan (Kang et al., 2001; Kim et al., 2012; Jung et al., 2013). It is a perennial brown alga belonging to the family Lessoniaceae, which has been previously reported to generate various metabolites such as phlorotannins (eckol, dieckol, phlorofucofuroeckol A, bieckols, and phloroeckols), sterols (fucosterol, saringosterol, and 24-ketocholesterol), and carotenoid (fucoxanthin) (Kim et al., 2011; Kim et al., 2013; Kurata et al., 1990; Moon et al., 2011; Negara et al., 2021; Okeke et al., 2021). Phlorotannins (polyphenolic compounds) are commonly polymerized by 1,3,5-trihydrobenzene (phloroglucinol) and are classified into six subclasses (phloroethols, fucols, eckols, carmalols, fucophloroehols, and fuhalols) (Chen et al., 2021; Duan et al., 2023; Go et al., 2024). They are key bioactive substances originated from *E. bicyclis* (Sugiura et al., 2021). These metabolites have been shown to possess potent bio-activities including anti-inflammatory, anti-oxidant, anti-viral, anti-diabetic, anti-cancer, and anti-microbial activities (Khan et al., 2022; Lee & Jeon, 2013; Lemesheva et al., 2023; Maheswari & Babu, 2022; Pradhan & Ki, 2023; Shin et al., 2014). In this current paper, we focus on the isolation, structural

Received: Jan 15, 2026 **Revised:** Feb 2, 2026 **Accepted:** Feb 9, 2026
[#]These authors contributed equally to this work.
***Corresponding author:** Jeong Min Lee, Ji-Yul Kim
National Marine Biodiversity Institute of Korea, Seocheon 33662, Korea
Tel: +82-41-950-0940, **E-mail:** lshjm@mabik.re.kr, jiyul2224@mabik.re.kr

determination, quantification, and anti-inflammatory activity of four oxylipin derivatives (1–4, Fig. 1) obtained from 70% ethanol extract of *E. bicyclis*.

Materials and Methods

General experimental procedures

Nuclear magnetic resonance (NMR) spectra were recorded using a VNMRS 500 MHz Fourier-transform nuclear magnetic resonance (FT-NMR) spectrometer (Varian, Palo Alto, CA, USA). The high-resolution quadrupole time-of-flight mass spectrometry (HR-Q-TOF-MS) spectra were obtained using a SCIEX X500R quadrupole time-of-flight (Q-TOF) liquid chromatography–tandem mass spectrometry (LC-MS/MS) spectrometer (SCIEX, Marlborough, MA, USA). High-performance liquid chromatography (HPLC) was performed using Waters ACQUITY Arc HPLC system (Waters, Milford, MA, USA). All chemical solvents were obtained by HPLC grades (J.T.baker, Radnor, PA, USA).

Plant materials

The brown alga, *E. bicyclis* was obtained from Jindo-gun, Jeallanam-do, Republic of Korea. A voucher specimen has been deposited at the National Marine Biodiversity Institute of Korea (MABIK).

Extraction and isolation

The brown alga *E. bicyclis* was washed and freeze-dried, subsequently, the dried *E. bicyclis* (400 g) was ground and extracted three times with 70% ethanol (2 L) at 50℃ for 4 hours. The extracts were filtered and partitioned using *n*-hexane, chloroform, ethyl acetate (EtOAc), and *n*-butanol. The *n*-hexane soluble portion (3 g) was subjected to flash silica gel column chromatography eluted with the gradient solvent system of *n*-hexane and EtOAc to obtain 12 fractions (S1–S12). The S7 fraction (*n*-hexane:EtOAc = 1:1, 174.1 mg) was further purified by preparative-HPLC (YMC pack C_{18} 10 mm × 250 mm, flow rate: 2 mL/min; YMC, Kyoto, Japan) using a stepwise gradient system of acetonitrile (ACN) and water (10% ACN → 50% ACN) to yield four compounds 1 (6.0 mg), 2 (4.2 mg), 3 (3.4 mg), and 4 (1.8 mg).

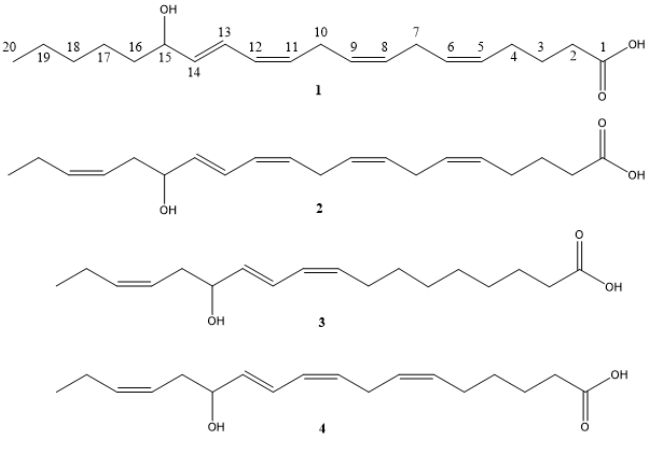

Fig. 1. Structures of compounds 1–4.

(5*Z*,8*Z*,11*Z*,13*E*)-15-hydroxyicosa-5,8,11,13-tetraenoic acid (1): yellow amorphous gum; high-resolution electrospray ionization mass spectrometry (HRESIMS): *m/z* 319.2260 $[M-H]^-$, calcd for $C_{20}H_{31}O_3$, 319.2271; ^{1}H NMR (500 MHz, CD_3OD) and ^{13}C NMR (125 MHz, CD_3OD) spectra were shown Table 1.

(5*Z*,8*Z*,11*Z*,13*E*,17*Z*)-15-hydroxyicosa-5,8,11,13,17-pentaenoic acid (2): yellow amorphous gum; HRESIMS: *m/z* 317.2109 $[M-H]^-$, calcd for $C_{18}H_{29}O_3$, 317.2116; ^{1}H NMR (500 MHz, CD_3OD) and ^{13}C NMR (125 MHz, CD_3OD) spectra were shown Table 1.

(9*Z*,11*E*,15*Z*)-13-hydroxyoctadeca-9,11,15-trienoic acid (3): yellow amorphous gum; HRESIMS: *m/z* 293.2112 $[M-H]^-$, calcd for $C_{18}H_{29}O_3$, 293.2116; ^{1}H NMR (500 MHz, CD_3OD) and ^{13}C NMR (125 MHz, CD_3OD) spectra were shown Table 1.

(6Z,9Z,11*E*,15*Z*)-13-hydroxyoctadeca-6,9,11,15-tetraenoic acid (4): yellow amorphous gum; HRESIMS: *m/z* 291.1948 $[M-H]^-$, calcd for $C_{18}H_{27}O_3$, 291.1960; ^{1}H NMR (500 MHz, CD_3OD) and ^{13}C NMR (125 MHz, CD_3OD) spectra were shown Table 1.

Determination of cell viability and nitric oxide (NO) production

RAW 264.7 macrophage cells were cultured in Dulbecco's modified Eagle's medium (DMEM) supplemented with 10% (v/v) fetal bovine serum (FBS), 1% penicillin/streptomycin in a 5% CO_2 incubator. The RAW 264.7 cells were seeded at 3×10^5 cells/mL in each well and added with lipopolysaccharide (1 μg/mL) and compounds 1–4 at 37℃ for 1 day. Cell viability was confirmed using cell counting kit-8 and recorded using microplate reader at the absorbance of 470 nm. NO production was measured using Griess Reagent Kit and microplate reader at absorbance of 548 nm.

Multiple reaction monitoring quantification using high-resolution electrospray ionization quadrupole time-of-flight (HR-ESI-Q-TOF) mass spectrometry

Compounds 1–4 were dissolved in methanol (liquid chroma-

Table 1. ^{1}H and ^{13}C NMR spectroscopic data for compounds 1–4 in CD_3OD[a] (δ in ppm, *J* in Hz)

No.	1		2		3		4	
	δ_C	δH (*J* in Hz)	δ_C	δH (*J* in Hz)	δ_C	δ_H (*J* in Hz)	δ_C	δ_H (*J* in Hz)
1	177.9		178.1		N.D		N.D	
2	34.6	2.29, t (7.2)	34.8	2.29, m	35.7	2.26, m	36.3	2.26, t (7.2)
3	26.2	1.66, p (7.2)	26.2	1.66, p (7.4)	26.5	1.60, m	26.3	1.62, p (7.5)
4	27.7	2.14, q (7.2)	27.7	2.12, m	30.2	1.33, m	30.5	1.42, p (7.5)
5	130.3	5.39, m	130.3	5.36, m	30.4	1.33, m	28.1	2.11, q (7.5)
6	129.9	5.37, m	129.8	5.36, m	30.4	1.33, m	131.3	5.40, m
7	26.6	2.84, m	26.6	2.84, m	30.8	1.40, m	128.8	5.37, m
8	128.8	5.37, m	128.8	5.36, m	28.7	2.19, m	27.1	2.94, t (7.3)
9	129.7	5.37, m	129.7	5.36, m	133.2	5.41, m	131.0	5.37, m
10	27.1	2.97, m	27.1	2.98, m	129.4	5.97, t (11.0)	129.3	5.98, t (11.0)
11	130.7	5.37, m	130.8	5.36, m	126.8	6.50, dd (15.1, 11.0)	126.5	6.55, dd (15.2, 11.0)
12	129.5	5.99, t (10.9)	129.4	5.98, t (10.9)	136.7	5.64, dd (15.1, 6.4)	137.3	5.67, dd (15.2, 6.5)
13	126.3	6.55, dd (15.2, 10.9)	126.5	6.56, dd (15.3, 11.0)	73.4	4.11, q (6.4)	73.3	4.12, q (6.5)
14	138.0	5.65, dd (15.2, 6.7)	137.4	5.68, dd (15.3, 6.5)	36.3	2.30, m	36.3	2.30, m
15	73.4	4.09, m	73.3	4.13, m	125.6	5.38, m	125.6	5.38, m
16	38.5	1.49, m	36.3	2.29, m	134.7	5.46, m	134.7	5.46, m
17	26.4	1.35, m	125.6	5.38, m	21.8	2.06, p (7.5)	21.8	2.06, p (7.5)
18	33.1	1.31, m	134.7	5.46, dt (10.4, 7.1)	14.7	0.96, t (7.5)	14.6	0.96, t (7.5)
19	23.8	1.32, m	21.8	2.05, p (7.5)				
20	14.6	0.91, t (6.7)	14.7	0.96, t (7.5)				

[a] NMR spectra were recorded at 500 MHz for 1H and 125 MHz for 13C.
NMR, nuclear magnetic resonance; N.D, not detected due to low intensity signal.

tography–mass spectrometry [LC-MS] grade). The concentrations of the stock solutions of 1–4 were 1 mg/mL. The calibration curve was generated using five points, with concentrations ranging from 6.25 to 200 ppm. The ground sample of *E. bicyclis* (10 g) was extracted with 70% ethanol at 70℃ for 4 hours. The extract was filtered and concentrated using an evaporator, and the sample solution was prepared at a concentration of 10 mg/mL and diluted to 1 mg/mL using methanol. The solution was filtered through a polytetrafluoroethylene (PTFE) syringe filter (pore size: 0.2 mm) for quantitative analysis. An ultra-performance liquid chromatography (UPLC) system equipped with an ACQUITY bridged ethylene hybrid (BEH) C_{18} column (2.1 mm × 100 mm, 1.7 mm) was used to separate the components from the extract. The mobile phase was used a binary solvent system consisting of acetonitrile (A line) and water in 0.1% formic acid (B line). The flow rate was 0.4 mL/min, and injection volume was 10 μL. The gradient elution was performed as follows: 0–2 min: 10% ACN, 2–9 min: 10%–20% ACN, 9–13 min: 20%–30% ACN, 13–16 min: 30%–40% ACN, 16–19 min: 40%–50% ACN, 19–22 min: 50%–70% ACN, 22–24.1 min: 70%–100% ACN, 24.1–26.0 min: 100% ACN, 26.0–26.2 min: 100%–10% ACN, 26.2–30.0 min: 10% ACN. Q-TOF-MS was performed in the negative ion mode using the following parameters: temperature: 500℃, CAD gas: 7, declustering potential at 80 V, collision energy at –30 V, CE spread at 15 V, spray voltage: –4,500 V, mass range: 100 Da to 1,000 Da.

Results and Discussion

Compound 1 was obtained as a yellow amorphous gum. The molecular formula of 1 was confirmed by high-resolution electrospray ionization mass spectrometry (HR-ESI-MS) based on a negative ion peak at *m/z* 319.2260 $[M-H]^-$ (calcd for $C_{20}H_{31}O_3$, 319.2271). The ^{13}C NMR spectrum of 1 showed the presence of a carbonyl carbon at d_c 177.9, four double bonds at d_c 138.0, 130.7, 130.3, 129.9, 129.7, 129.5, 128.8, 126.3, one oxygenated carbon at d_c 73.4, nine methylene carbons at d_c 38.5, 34.6, 33.1, 27.7, 27.1, 26.6, 26.4, 26.2, 23.8, and one methyl carbon at d_c 14.5 (Table 1). The key HMBC correlations from H-20 (δ_H 0.91) to C-18 (δ_C 33.1), C-19 (δ_C 23.8), from H-15 (δ_H 4.09) to C-13 (δ_C 126.3), C-14 (δ_C 138.0), C-16 (δ_C 38.5), C-17 (δ_C 26.4), from H-13 (δ_H 6.55) to C-11 (δ_C 130.7), C-12 (δ_C 129.5), C-15 (δ_C 73.4), from H-10 (δ_H 2.97) to C-8 (δ_C 128.8), from H-7 (δ_H 2.84) to C-6 (δ_C 129.9) indicated that oxygenated aliphatic skeleton including four olefinic methines. Furthermore, the HMBC correlations from H-2 (δ_H 2.29) to C-1 (δ_C 177.9), from H-3 (δ_H 1.66) to C-1 (δ_H 177.9), C-2 (δ_H 34.6), C-4 (δ_H 27.7) suggested the butyric acid moiety. The connectivity between aliphatic skeleton and butyric acid was elucidated by

https://doi.org/10.47853/FAS.2026.e45

^{1}H-^{1}H correlation spectroscopy (COSY) correlation with H-4 (δ_H 2.14)/H-5 (δ_H 5.39). The geometries at H-13 (δ_H 6.55, dd, *J* = 15.2, 10.9 Hz)/H-14 (δ_H 5.65, dd, *J* = 15.2, 6.7 Hz), H-12 (δ_H 5.99, t, 10.9 Hz)/H-13 (δ_H 6.55, dd, *J* = 15.2, 10.9 Hz), H-11 (δ_H 5.37)/H-12 (δ_H 5.99, t, 10.9 Hz) indicated that the presence of *E*-form (*J* = 15.2 Hz, H-13), *Z*-form (*J* = 10.9 Hz, H-12), and *Z*-form (*J* = 10.9 Hz, H-11) due to ^{1}H NMR coupling constants. Furthermore, H-8 (δ_H 5.37)/H-9 (δ_H 5.37) and H-5 (δ_H 5.37)/H-6 (δ_H 5.39) tentatively suggested that *Z*-form due to similar ^{1}H and ^{13}C NMR spectra of arachidonic acid (Fu et al., 2004). Therefore, compound 1 was identified as (5*Z*,8*Z*,11*Z*,13*E*)-15-hydroxyicosa-5,8,11,13-tetraenoic acid.

Compound 2 was obtained in the form of a yellow amorphous gum. Its molecular formula was determined to be $C_{20}H_{30}O_3$ based on negative HR-ESI-MS ion peak at *m/z* 317.2109 $[M-H]^-$ (calcd for $C_{20}H_{29}O_3$, 317.2116). The ^{1}H and ^{13}C NMR spectra of 1 were indicated that the presence of carbonyl (d_c 178.1), five olefinic methines (δ_H 6.56, 5.98, 5.68, 5.46, 5.36-5.38/d_c 137.4, 134.7, 130.8, 130.3, 129.8, 129.7, 129.4, 128.8, 126.5, 125.6), oxygenated methine (δ_H 4.13/δ_C 73.3), seven methylenes (δ_H 1.66, 2.05, 2.12, 2.29, 2.29, 2.84, 2.98/d_c 21.8, 26.2, 26.6, 27.1, 27.7, 34.8, 36.3), and methyl (δ_H 0.96/d_c 14.7) (Table 1). Compound 2 was similar to those of 1, except for the presence of olefin at H-17 (δ_H 5.38)/H-18 (δ_H 5.46) instead of single bond at H-17 (δ_H 1.35)/H-18 (δ_H 1.31) in 1 due to heteronuclear multiple bond correlation (HMBC) correlations from H-19 (δ_H 2.05) to C-17 (δ_C 125.6), C-18 (δ_C 134.7), H-15 (δ_H 4.13) to C-16 (δ_C 36.3), C-17 (δ_C 125.6). The geometry at H-17 (δ_H 5.38)/H-18 (δ_H 5.46) was elucidated to be *Z*-form by ^{1}H NMR coupling constant at H-18 (δ_H 5.48, dt, *J* = 10.4, 7.1 Hz). Thus, compound 2 was elucidated as (5*Z*,8*Z*,11*Z*,13*E*,17*Z*)-15-hydroxyicosa-5,8,11,13,17-pentaenoic acid.

Compound 3 was obtained as a yellow amorphous gum, and its molecular formula was assigned to be $C_{18}H_{30}O_3$ by HR-ESI-MS, based on a negative ion peak at *m/z* 293.2112 $[M-H]^-$ (calcd for $C_{18}H_{29}O_3$, 293.2116). The 1D NMR spectra of 3 was exhibited the signals at three olefinic methines (δ_H 6.50, 5.97, 5.64, 5.46, 5.41, 5.36/δ_C 136.7, 134.7, 133.2, 129.4, 126.8, 125.6), nine methylenes (δ_H 1.33, 1.33, 1.33, 1.40, 1.60, 2.06, 2.19, 2.26, 2.30/δ_C 21.8, 26.5, 28.7, 30.2, 30.4, 30.4, 30.8, 36.3), oxygenated methine (δ_H 4.11/δ_C 73.4), and methyl (δ_H 0.96/δ_C 14.7). However, the carbonyl carbon (C-1) was not detected because of limited amount (Table 1). The main difference between 2 and 3 was the absence of a single bond and double bond. The key evidences were confirmed by HMBC correlations from H-8 (δ_H 2.19) to C-7 (δ_C 30.8), and H-2 (δ_H 2.26) to C-3 (δ_C 26.5), C-4 (δ_C 30.2) and ^{1}H-^{1}H COSY correlations with H-6 (δ_H 1.33)/H-7 (δ_H 1.40) and H-3 (δ_H 1.60)/H-4 (δ_H 1.33). The geometries at three double bonds were determined to be *Z*- forms at H-9 (δ_H 5.41, m)/H-10 (δ_H 5.97, t, *J* = 11.0 Hz) and H-15 (δ_H 5.36, m)/H-16 (δ_H 5.46, m), and *E*-form at H-11 (δ_H 6.50, dd, *J* = 15.1, 11.0 Hz)/H-12 (δ_H 5.64, dd, *J* = 15.1, 6.4 Hz) by ^{1}H NMR coupling constants and comparing with 2. Therefore, compound 3 was elucidated as (9*Z*,11*E*,15*Z*)-13-hydroxyoctadeca-9,11,15-trienoic acid.

Compound 4 was also obtained as a yellow amorphous gum. Its molecular formula was determined to be $C_{18}H_{28}O_3$ using HR-ESI-MS, based on a negative ion peak at *m/z* 291.1948 (calcd for $C_{18}H_{27}O_3$, 291.1960). The ^{1}H and ^{13}C NMR spectra (Table 1) of 4 were similar to those of 3 except for the replacement of the double bond at H-6 (δ_H 5.40)/H-7 (δ_H 5.37) with single bond at H-6 (δ_H 1.33)/H-7 (δ_H 1.40). However, the carbonyl carbon was not detected due to low intensity. The double bond at H-6 (δ_H 5.40)/H-7 (δ_H 5.37) was elucidated by HMBC correlations from H-4 (δ_H 1.42) to C-6 (δ_C 131.3), from H-5 (δ_H 2.11) to C-6 (δ_C 131.3), C-7 (δ_C 128.8), and from H-8 (δ_H 2.94) to C-6 (δ_C 131.3), C-7 (δ_C 128.8). The ^{1}H and ^{13}C NMR signals at H-2 (δ_H 2.26)/C-2 (δ_C 36.3) in 4 suggested the presence of a carbonyl group, in comparison to the proton and carbon NMR signals at δ_H 2.29/δ_C 34.6 in 1. The geometries at double bonds were determined to be *Z*-form (H-6), *Z*-form (H-9), *E*-form (H-11), and *Z*-form (H-15) by comparison of NMR evidence in 1–3. Accordingly, compound 4 was determined to be (6*Z*,9*Z*,11*E*,15*Z*)-13-hydroxyoctadeca-6,9,11,15-tetraenoic acid. The MS chromatograms were obtained using HR-Q-TOF-MS spectroscopy. Compounds 1–4 were detected at 21.2–22.5 min. The main product ions for compounds 1–4 were delected at *m/z* 257.2232 $[M-H]^-$, 255.2102 $[M-H]^-$, 195.1374 $[M-H]^-$, and 193.1215 $[M-H]^-$ respectively (Fig. 2). The calibration curves and correlation coefficients (R^2) are summarized in Table 2. The concentrations of compounds 1–4 in the 70% ethanol extract of *E. bicyclis* were confirmed to be 0.060 mg/g in 1, 0.155 mg/g in 2, 0.042 mg/g in in 3, and 0.161 mg/g in 4, respectively (Table 2). The cell viability of compounds 1–4 exhibited their non-toxicity at a concentration of 100 mg/mL. We evaluated the inhibitory activity of compounds 1–4 on NO production at the concentrate of 100 mg/mL. The effects of compounds 1–4 on NO production at 100 μg/mL are shown in Fig. 3.

Conclusion

This study describes the isolation, structural identification, and

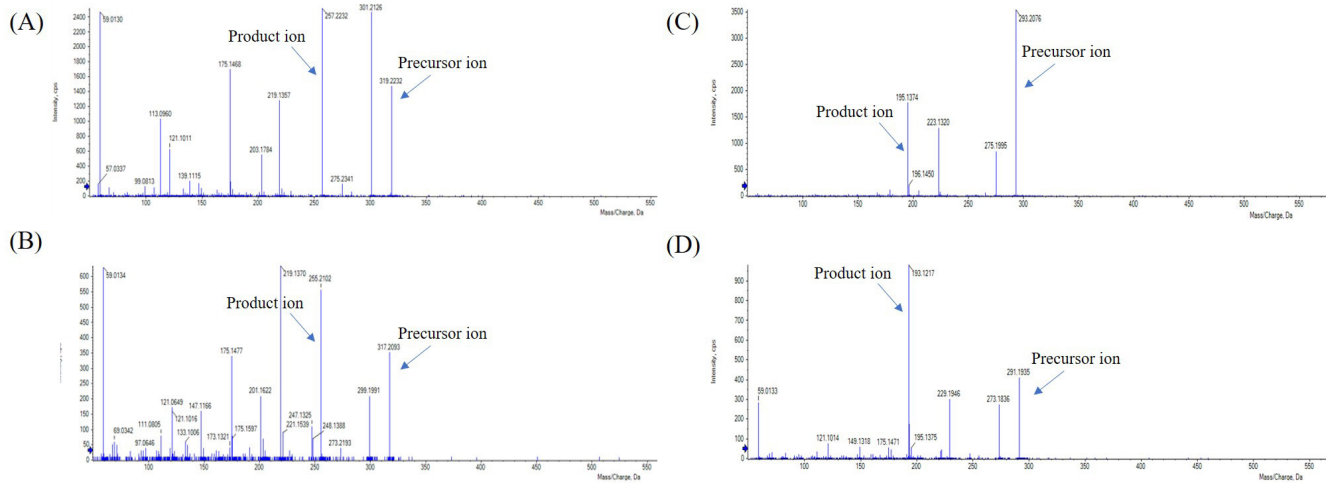

Fig. 2. Liquid chromatography–tandem mass spectrometry (LC-MS/MS) chromatograms of compounds 1–4.

Table 2. The MRM quantification analysis of compounds 1–4 using HR-Q-TOF mass spectroscopy

Compounds	R.T (min)	Calibration curve	R^2	Amount (mg/g)	LOD	LOQ
1	22.5	y = 4.45286x + 325.79208	0.998	0.060 ± 0.003	0.002	0.008
2	21.9	y = 0.78074x + 41.48428	0.995	0.155 ± 0.009	0.039	0.118
3	21.6	y = 11.20742x + 244.39414	0.999	0.042 ± 0.003	0.001	0.003
4	21.1	y = 0.80093x + 17.26867	0.997	0.161 ± 0.003	0.016	0.049

MRM, multiple reaction monitoring; HR-Q-TOF, high-resolution quadrupole time-of-flight; R.T, retention time; LOD, limit of detect; LOQ, limit of quantification.

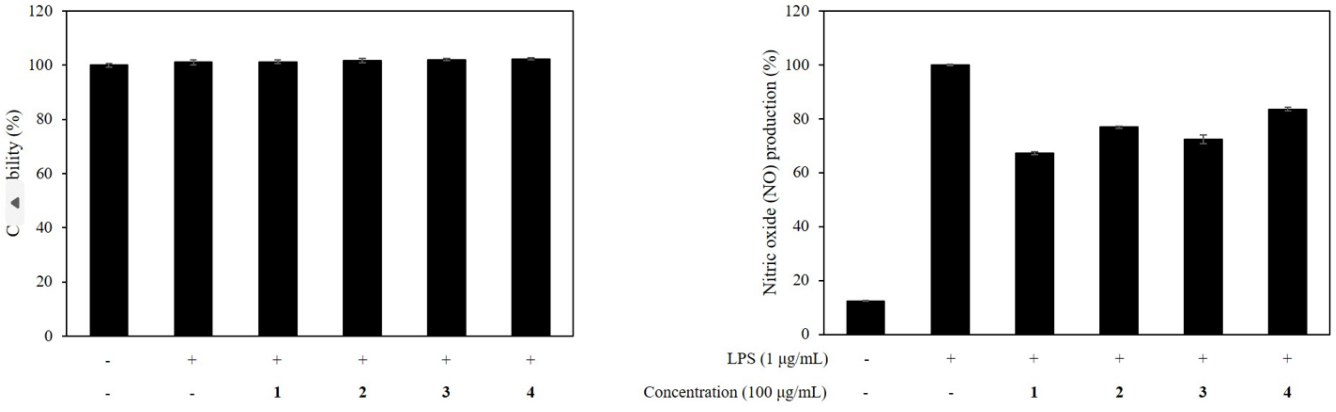

Fig. 3. Effects of compounds 1–4 on the cell viability and the production of nitric oxide (NO) in the lipopolysaccharide (LPS)-induced RAW 264.7 cells at a concentration of 100 μg/mL.

quantification of four known oxylipin derivatives from *E. bicyclis*. All compounds were determined to be (5*Z*,8*Z*,11*Z*,13*E*)-15-hydroxyicosa-5,8,11,13-tetraenoic acid (1), (5*Z*,8*Z*,11*Z*,13*E*,17*Z*)-15-hydroxyicosa-5,8,11,13,17-pentaenoic acid (2), (9*Z*,11*E*,15*E*)-13-hydroxyoctadeca-9,11,15-trienoic acid (3), and (6*Z*,9*Z*,11*E*,15*Z*)-13-hydroxyoctadeca-6,9,11,15-tetraenoic acid (4), respectively. Furthermore, four oxylipin derivatives from the 70% EtOH extract of *E. bicyclis* were evaluated for their anti-inflammatory activities. The results showed the level of NO production were significantly inhibited at the concentration of 100 mg/mL. Quantitative analysis of compounds 1–4 revealed the following contents: 0.060 ± 0.003 mg/g (1), 0.155 ± 0.003 mg/g (2), 0.042 ± 0.003 mg/g (3), and 0.161 ± 0.009 mg/g (4). Phlorotannins have been reported as the major bioactive compounds in the brown alga *E. bicyclis*. In contrast, the present study demonstrates that oxylipin derivatives also contribute

https://doi.org/10.47853/FAS.2026.e45

to the biological profile of this species, with the primary focus on the quantitative characterization of four known oxylipins (1–4) in the 70% ethanol extract, accompanied by a preliminary evaluation of their NO inhibitory activity at a concentration of 100 μg/mL. Among the identified oxylipins, compound 4 was found to be the most abundant. Furthermore, oxylipins from *E. bicyclis* were reported to have anti-microbial activities against two strains. Oxylipins are oxidized polyunsaturated fatty acid derivatives, which has been reported to regulate a wide range of biological functions (Ağagündüz et al., 2024; Barbosa et al., 2016; Misheva et al., 2022). These findings indicate that diverse biological activities of *E. bicyclis* could be attributed to both phlorotannins and oxylipins. Taken together, these results suggest that the biological activities of *E. bicyclis* may arise from multiple classes of metabolites, highlighting its potential as a source of anti-inflammatory bioactive compounds.

Supplementary Materials

Supplementary materials are only available online from: https://doi.org/10.47853/FAS.2026.e45

Competing interests

No potential conflict of interest relevant to this article was reported.

Funding sources

This research was supported by the Department of Biomaterial Research, National Marine Biodiversity Institute of Korea Research Program (2026M00500).

Acknowledgements

Not applicable.

Availability of data and materials

Not applicable.

Ethics approval and consent to participate

Not applicable.

ORCID

Gun-Woo Oh https://orcid.org/0000-0003-0494-2508
Soo Jeong Lee https://orcid.org/0009-0007-3127-5938
Dae-Cheol Choi https://orcid.org/0009-0003-7664-5454
Seok-Chun Ko https://orcid.org/0000-0002-0509-3336
Dongwoo Yang https://orcid.org/0000-0002-7335-2352
Mi-Jin Yim https://orcid.org/0000-0002-2086-1823
Dae-Sung Lee https://orcid.org/0000-0003-0627-1402
Jeong Min Lee https://orcid.org/0000-0002-9593-1849
Ji-Yul Kim https://orcid.org/0000-0002-9638-7179

References

Ağagündüz D, Yeşildemir Ö, Koçyiğit E, Koçak T, Özen Ünaldı B, Ayakdaş G, et al. Oxylipins derived from PUFAs in cardiometabolic diseases: mechanism of actions and possible nutritional interactions. Nutrients. 2024;16:3812.

Barbosa M, Valentão P, Andrade PB. Biologically active oxylipins from enzymatic and nonenzymatic routes in macroalgae. Mar Drugs. 2016;14:23.

Chen L, Liu R, He X, Pei S, Li D. Effects of brown seaweed polyphenols, a class of phlorotannins, on metabolic disorders via regulation of fat function. Food Funct. 2021;12:2378-88.

Duan X, Agar OT, Barrow CJ, Dunshea FR, Suleria HAR. Improving potential strategies for biological activities of phlorotannins derived from seaweeds. Crit Rev Food Sci Nutr. 2023;65:833-55.

Fu M, Koulman A, van Rijssel M, Lützen A, Karin de Boer M, Tyl MR, et al. Chemical characterisation of three haemolytic compounds from the microalgal species *Fibrocapsa japonica* (Raphidophyceae). Toxicon. 2004;43:355-63.

Go YG, Wang Q, Park J, Lee HJ, Kim H. Phlorotannins isolated from *Eisenia bicyclis* and *Lactobacillus casei* ameliorate dextran sulfate sodium-induced colitis in mice through the AhR pathway. Appl Sci. 2024;14:2835.

Jung HA, Jin SE, Ahn BR, Lee CM, Choi JS. Anti-inflammatory activity of edible brown alga *Eisenia bicyclis* and its constituents fucosterol and phlorotannins in LPS-stimulated RAW264.7 macrophages. Food Chem Toxicol. 2013;59:199-206.

Kang RS, Won KS, Hong KP, Kim JM. Population studies on the kelp *Ecklonia cava* and *Eisenia bicyclis* in Dokdo, Korea. Algae. 2001;16:209-15.

Khan F, Jeong GJ, Khan MSA, Tabassum N, Kim YM. Seaweed-derived phlorotannins: a review of multiple biological roles and action mechanisms. Mar Drugs. 2022;20:384.

Kim KA, Kim SM, Kang SW, Jeon SI, Um BH, Jung SH. Edible seaweed, *Eisenia bicyclis*, protects retinal ganglion cells death caused by oxidative stress. Mar Biotechnol. 2012;14:383-95.

Kim SM, Kang SW, Jeon JS, Jung YJ, Kim WR, Kim CY, et al. Determination of major phlorotannins in *Eisenia bicyclis* using hydrophilic interaction chromatography: seasonal variation and extraction characteristics. Food Chem. 2013;138:2399-406.

Kim SM, Shang YF, Um BH. A preparative method for isolation of fucoxanthin from *Eisenia bicyclis* by centrifugal partition chromatography. Phytochem Anal. 2011;22:322-9.

Kurata K, Taniguchi K, Shiraishi K, Suzuki M. A C26 sterol from the brown alga *Eisenia bicyclis*. Phytochemistry. 1990;29:3678-80.

Lee SH, Jeon YJ. Anti-diabetic effects of brown algae derived phlorotannins, marine polyphenols through diverse mechanisms. Fitoterapia. 2013;86:129-36.

Lemesheva V, Islamova R, Stepchenkova E, Shenfeld A, Birkemeyer C, Tarakhovskaya E. Antibacterial, antifungal and algicidal activity of phlorotannins, as principal biologically active components of ten species of brown algae. Plants. 2023;12:821.

Maheswari V, Babu PA. Phlorotannin and its derivatives, a potential antiviral molecule from brown seaweeds, an overview. Russ J Mar Biol. 2022;48:309-24.

Misheva M, Johnson J, McCullagh J. Role of oxylipins in the inflammatory-related diseases NAFLD, obesity, and type 2 diabetes. Metabolites. 2022;12:1238.

Moon HE, Islam MN, Ahn BR, Chowdhury SS, Sohn HS, Jung HA, et al. Protein tyrosine phosphatase 1B and α-glucosidase inhibitory phlorotannins from edible brown algae, *Ecklonia stolonifera* and *Eisenia bicyclis*. Biosci Biotechnol Biochem. 2011;75:1472-80.

Negara BFSP, Sohn JH, Kim JS, Choi JS. Antifungal and larvicidal activities of phlorotannins from brown seaweeds. Mar Drugs. 2021;19:223.

Okeke ES, Nweze EJ, Chibuogwu CC, Anaduaka EG, Chukwudozie KI, Ezeorba TPC. Aquatic phlorotannins and human health: bioavailability, toxicity, and future prospects. Nat Prod Commun. 2021;16.

Pradhan B, Ki JS. Antioxidant and chemotherapeutic efficacies of seaweed-derived phlorotannins in cancer treatment: a review regarding novel anticancer drugs. Phytother Res. 2023;37:2067-91.

Shin T, Ahn M, Hyun JW, Kim SH, Moon C. Antioxidant marine algae phlorotannins and radioprotection: a review of experimental evidence. Acta Histochem. 2014;116:669-74.

Sugiura Y, Katsuzaki H, Imai K, Amano H. The anti-allergic and anti-inflammatory effects of phlorotannins from the edible brown algae, *Ecklonia* sp. and *Eisenia* sp. Nat Prod Commun. 2021;16.

https://doi.org/10.47853/FAS.2026.e45